Static Behavior of 40 Year-Old Prestressed Concrete Bridge Girders Strengthened with Various FRP Systems

O.A. Rosenboom, R. O. Carneiro, T.K. Hassan, A. Mirmiran & S.H. Rizkalla
North Carolina State University, Raleigh, NC, USA

ABSTRACT: This paper presents preliminary experimental results of a research program aimed at investigating the static behavior of 40 year-old prestressed concrete bridge girders strengthened with various Carbon Fiber Reinforced Polymer (CFRP) systems. Five 40 year old, 9.14m long, prestressed bridge girders have been tested: one control and four specimens strengthened with various CFRP systems. Test results showed that there is virtually no difference in behavior between the control and the strengthened specimens up to yielding of the prestressing strands, which occurred well after the expected service loading level of the bridge. The measured ultimate strength was increased according to the design value based on finite element analysis. The behavior of the tested specimens was predicted using non-linear finite element analysis. Excellent agreement was observed between the measured and the predicted behavior up to failure. Cost-effective analysis was also performed for various CFRP strengthening techniques. Comparing the percent increase in ultimate strength to the cost of the strengthening procedure, near surface mounted (NSM) technique has proven to be the most cost-effective system.

1 INTRODUCTION

1.1 *Research Objectives*

The primary objective of the research described in this paper is to provide the prestressed concrete industry as well as the departments of transportation with a value engineering and cost-effectiveness analysis of prestressed concrete bridge girders strengthened with various CFRP systems. The feasibility of using CFRP strengthening systems to upgrade the load carrying capacity of prestressed concrete bridges is investigated. Although there is an ever-expanding research database of reinforced concrete strengthened with different CFRP systems, the benefits of various strengthening techniques to prestressed concrete is limited (Hassan & Rizkalla 2002).

1.2 *Background*

The characterization of NSM strengthening systems with regards to performance has been well researched for reinforced concrete members (Hassan & Rizkalla 2002, De Lorenzis & Nanni 2001, De Lorenzis et al. 2000). It has been proven to be a viable, if not superior, alternative to externally bonded strengthening systems. With regards to prestressed concrete, externally bonded (EB) systems have been applied to aged prestressed girders (Takács & Kanstad 2000). NSM strengthening was carried out on prestressed slabs (Hassan & Rizkalla 2002). In both cases, performance gains were made with respect to ultimate load capacity. Debonding failure of externally bonded FRP systems were observed by many researchers most often at the termination point of the FRP strip/sheet for strengthened systems with a short span, and at the mid-span section for long span members. Many rational models predicting the failure loads of reinforced concrete members strengthened with FRP due to plate end debonding have been proposed (Smith and Teng 2001). Nevertheless, very little research work has been reported on the mid-span debonding mechanism (Wu & Niu 2000). Although of less concern in NSM systems, debonding models have been characterized from earlier plate-based work (Hassan & Rizkalla 2003).

2 EXPERIMENTAL PROGRAM

2.1 *Test Specimens*

As part of the extensive research program sponsored by North Carolina Department of Transportation, five 40 year old 9.14m long prestressed concrete bridge girders were tested at the Constructed Facilities Laboratory (CFL) at North Carolina State University (NCSU).

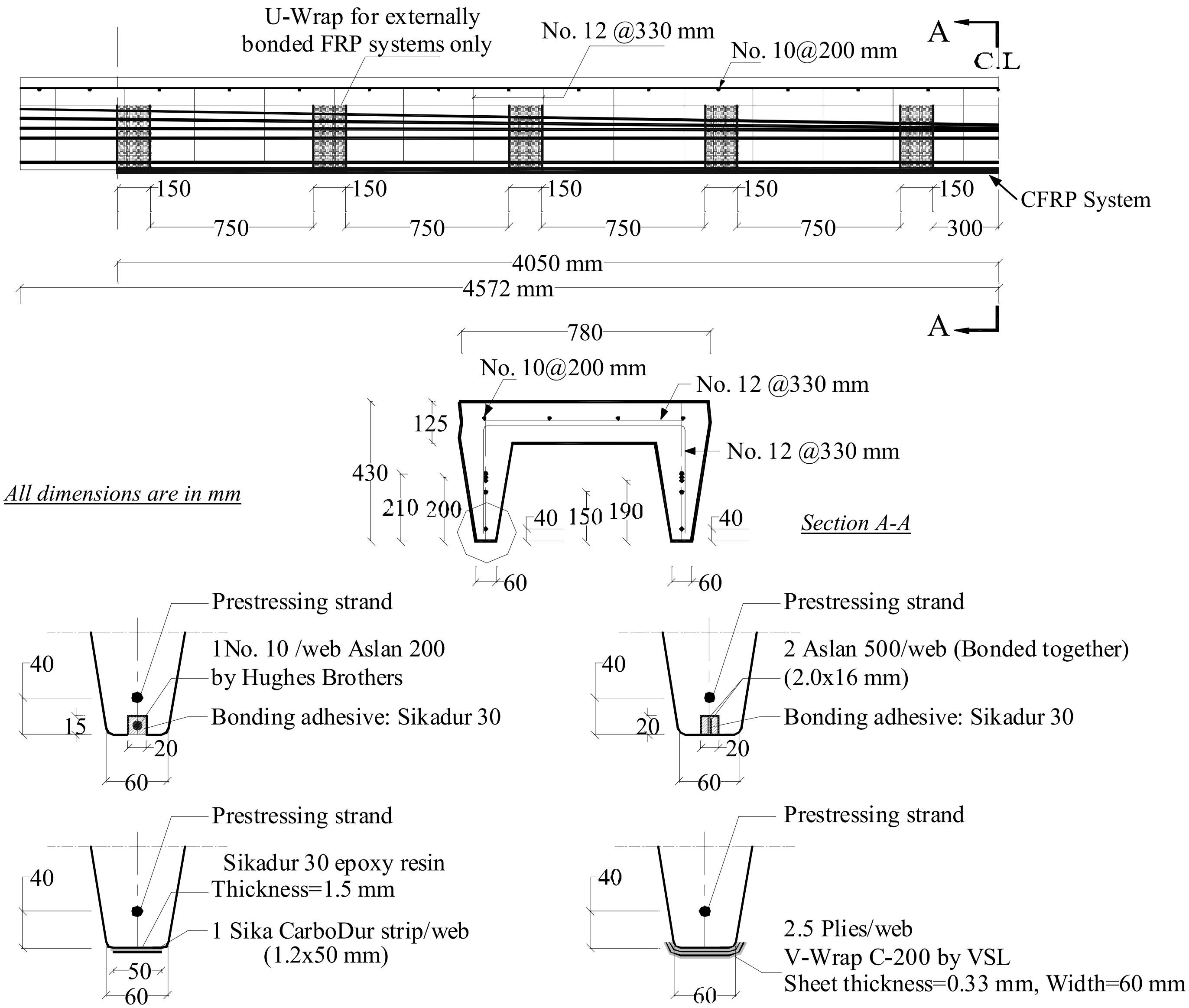

Figure 1. Plan and Cross-Section of C-Channel Girders

One specimen was tested as a control specimen, while the remaining four specimens were strengthened with NSM CFRP bars, strips and externally bonded CFRP strips and sheets. All five specimens were C-Channel type prestressed concrete bridge girders as shown in Figure 1. The girders were taken from the same bridge in Cartaret County, NC, USA, which was erected in 1961. The girders were in fair to good condition upon delivery. According to core samples tested per ASTM C42, the average compression strength of the concrete ranged from 48MPa to 74MPa. Each girder had ten 1725MPa seven-wire stress relieved prestressing strands (five in each web) and a 125mm deck with minimal reinforcing as shown in Figure 1. The wearing surface had been removed prior to delivery. The camber of the girders at mid-span due to prestressing and self weight was 40 mm.

Four different types of CFRP systems were applied to the two webs in each strengthened specimen: two were Externally Bonded (EB) and two were Near-Surface Mounted (NSM). Within the limits of the geometry of the supplied materials and specimen dimensions, they were all designed to achieve 30 percent increase in strength. The first EB system used one 50mm wide Sika CarboDur strip per web, bonded using SikaDur 30 adhesive. The second EB system used two and a half 50mm wide plies of VSL V-Wrap C-200 sheets per web bonded using VSL saturant. The first NSM system used one10mm Aslan 200 CFRP bar per web. The bars were provided by Hughes Brothers and were bonded using SikaDur 30 adhesive. The second NSM system used two 2mm×16mm Aslan 500 strips per web provided by Hughes Brothers. The strips were bonded together prior to strengthening using SikaDur 30 adhesive. The strips were bonded to concrete using the same adhesive.

For the two EB systems, 150mm wide U-wraps were provided at 900mm spacing along the length of the girder to control the debonding mechanism. Figure 1 shows the reinforcement details and Table 1 provides the material properties of the CFRP systems along with the groove dimensions.

Table 1. Material Properties of CFRP Strengthening Systems

System	A_{FRP}	E_{FRP}	f_{uFRP}	w_G*	d_G*
	mm^2	GPa	MPa	mm	mm
NSM Bars	130	124	2070	19	19
NSM Strips	130	131	2070	19	19
EB Strips	119	165	2800	-	-
EB Sheets	84	228	3790	-	-

* w_G and d_G are the width and depth of the NSM groove, respectively

2.2 *Design of Strengthened Specimens*

The design of the strengthened specimens proceeded after the testing of the control specimen. The objective of the strengthening was to achieve a 30 percent increase in the ultimate load carrying capacity in comparison to the control specimen. Each strengthened specimen was designed using a cracked section analysis program (Response 2000). The manufacturer's properties were used to model the FRP materials. The prestressing and mild steel reinforcing properties were taken from the provided specifications. The concrete strength was obtained from core samples. It was recognized that the EB systems are more prone to delamination compared to NSM systems. According to Malek et al. 1998, the shear stresses at the cut-off points of the CFRP sheets/strips were significantly less than the shear strength of the concrete. Therefore, plate-end debonding should not be a concern. To delay delamination-type failures along the length of the girder, 150mm wide U-wraps were provided at 900mm spacing. This arrangement of the U-wraps was selected to simulate typical anchorage details commonly used for reinforced concrete members.

2.3 *Test Setup / Instrumentation / Loading*

The girders were tested using a 490kN MTS hydraulic actuator mounted to a steel frame placed at the midspan of the girder. To simulate loading on an actual bridge, a set of truck tires filled with silicon rubber filler were used to apply the load from the actuator. The footprint of the two tires was approximately 250mm × 500mm per the AASHTO specified loading area (AASHTO 2003). The supports for the girders on either side included a 64mm thick neoprene pad, a 25mm thick steel plate and hydrostone used for leveling purposes. The width of the neoprene pads was 216mm, which yielded a clear span for the girder of 8710 mm.

The behavior of the girders during testing was monitored using a set of string potentiometers placed at midspan, quarter span and at the ends to measure the deformation in the neoprene pads. The compressive strain in the top concrete surface was measured using a combination of PI gauges and strain gauges placed around and between the loading tires. PI gauges were placed at the level of the lowest prestressing strands to measure the crack width. Six strain gauges were applied to the CFRP reinforcement. The specimens were loaded up to a load level of 20 kN and unloaded and then reloaded again up to failure with a rate of 2.5mm/min. This loading scenario was used to determine the effective prestressing force in the girders by observing the reopening of the flexural cracks (Zia & Kowalsky 2002). Based on test results, the effective prestressing per strand ranged between 67 to 80 kN. After yielding of the prestressing strands, the loading rate was increased to 5mm/min.

2.4 *Test Results – Control specimen*

All the tested girders were uncracked prior to testing. Cracking of the control specimen occurred at a load level of 61.5kN. Flexural cracks were evenly distributed along the length of the girder. It was observed that steel stirrups acted as crack initiators even for the strengthened specimens. Yielding of the prestressing strands took place at a load level of 115 kN based on the PI gauge readings. The specimen failed due to concrete crushing at a load 148kN with an ultimate displacement of 228mm. The average crack width at failure was 1.9mm according to the PI gauge readings on the tension face. Due to confinement effects at the loading zone, crushing occurred first at the edge of the girder at midspan slightly before it occurred underneath the loading tires. The load-deflection behavior as well as the load-concrete compressive strain behavior are shown in Figures 2 and 3, respectively. Both of these plots do not include the camber of the girder. The concrete compressive strain at failure, ε_{cu}, was 0.0029. Test results are summarized in Table 2.

Table 2. Summarized Test Results

System	f'_c	P_e	P_{ult}	P_{cr}	ε_{FRP}	ε_{cu}	I
	MPa	kN	kN	kN	mm/mm	mm/mm	%
Control	74	72	148	61.5	-	.0029	-
NSM Bars	66	80	181	55.0	.0137	.0036	22
NSM Strips	60	69	182	55.0	.0146	.0035	23
EB Strips	48	72	176	57.0	.0122	.0034	19
EB Sheets	51	67	163	57.0	.0117	.0026	10

where f'_c is average compressive strength of the concrete based on core tests; P_e is the measured effective prestressing force per strand; P_{ult} is the ultimate load carrying capacity of the test specimen; P_{cr} is the cracking load; ε_{FRP} is the maximum measured tensile strain in the FRP reinforcement at ultimate; ε_{cu} is the maximum measured compressive strain in the concrete at ultimate and I is the percentage increase in ultimate capacity compared to the control specimen.

2.5 *Test Results – Strengthened Specimens*

Test results for the strengthened systems are summarized in Table 2 and shown in Figures 2-4. Brief descriptions of each test are provided below.

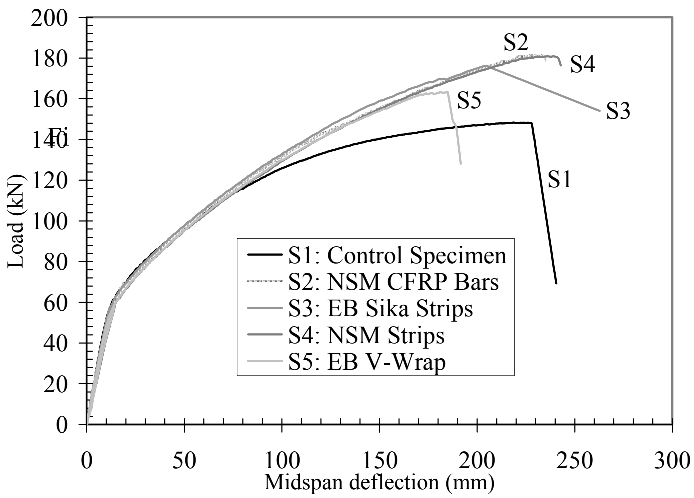

Figure 2. Load-deflection behavior of the test specimens

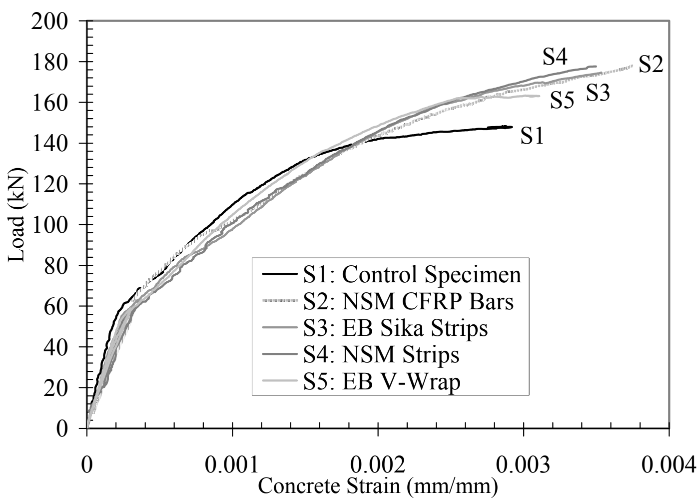

Figure 3. Load-concrete strain behavior of the test specimens

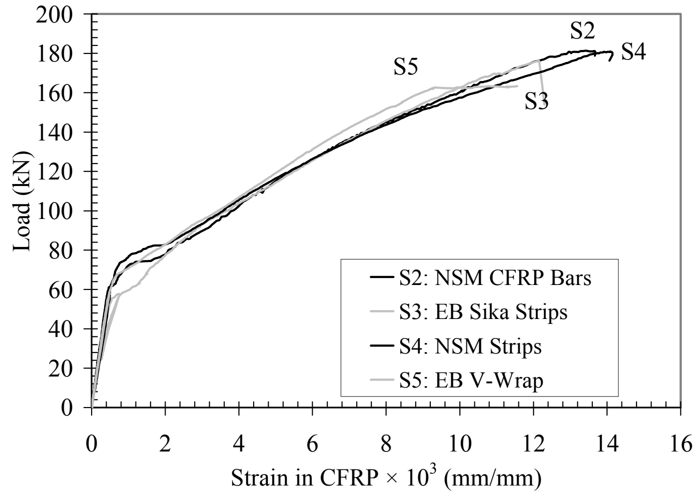

Figure 4. Load versus Tensile Strain in CFRP for Strengthened Specimens

2.5.1 *NSM CFRP Systems*

Both NSM Strengthened systems performed similarly during testing. Both specimens experienced flexural cracking at a load level of 55kN. The initial stiffness of the strengthened systems was identical to that of the control specimen, as was the post-cracking stiffness. After yielding of the prestressing strands, presence of the CFRP reinforcement constrains opening of the cracks and consequently reduced the deflection compared to the control specimen. The flexural cracks were spaced closer together than the control specimen. The failure of both girders strengthened with NSM CFRP reinforcement was due to concrete crushing followed by debonding of the NSM CFRP reinforcement at a load of 180kN for the NSM bars and 181kN for the NSM strips as shown in Figure 5. Since the ultimate strain in the concrete controlled the failure mode of both specimens, the curvature and consequently, the deflection at ultimate were very similar.

Figure 5. Typical failure due to concrete crushing of the specimens strengthened with NSM CFRP systems

Test results showed that strengthening of the prestressed girders using NSM CFRP bars and strips increased the ultimate load carrying capacity by 22 and 23 percent, respectively. The maximum measured tensile strain in the NSM CFRP bars and strips at failure was 81 and 86 percent of the manufactured rupture strain, respectively.

2.5.2 *EB CFRP Systems*

The performance of both prestressed concrete girders strengthened with externally bonded CFRP strips and sheets matched those strengthened with NSM systems and the control specimen before and after cracking. Flexural cracking at mid-span was observed at a load level of 57kN for both specimens. The flexural crack spacing was similar to that of the NSM systems up to failure. For the EB CFRP strips, failure occurred due to midspan debonding of the strips between the provided U-wraps at a load level of 176 kN. The debonded length extended 3700mm from midspan as shown in Figure 6.

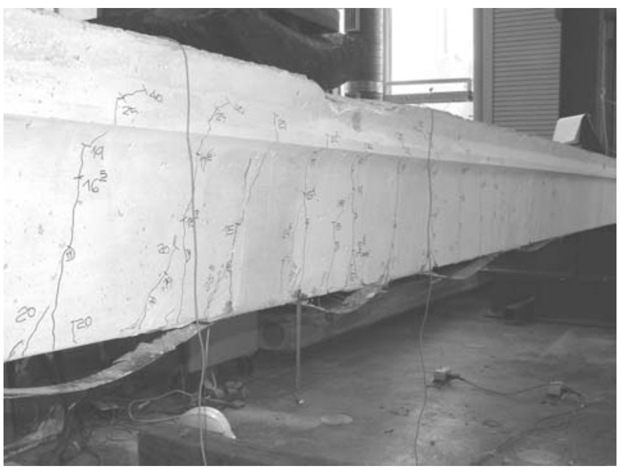

Figure 6. Debonding of externally bonded CFRP strips

Delamination occurred at the concrete substrate. However, in some areas debonding at the FRP-adhesive interface was observed possibly due to a poor bond during installation. For the EB CFRP sheets, failure was due to rupture of the sheets at midspan at a load of 163kN as shown in Figure 7. After failure it was also noted that the sheets had debonded over a distance of approximately 500mm from midspan. The maximum measured tensile strain in the CFRP sheets at failure was 1.17 percent, which is 70 percent of the manufacturer's guaranteed rupture strain. Compared to the control specimen, the EB CFRP strips and EB CFRP sheets achieved an increase in the ultimate load carrying capacity of 19 percent and 10 percent, respectively.

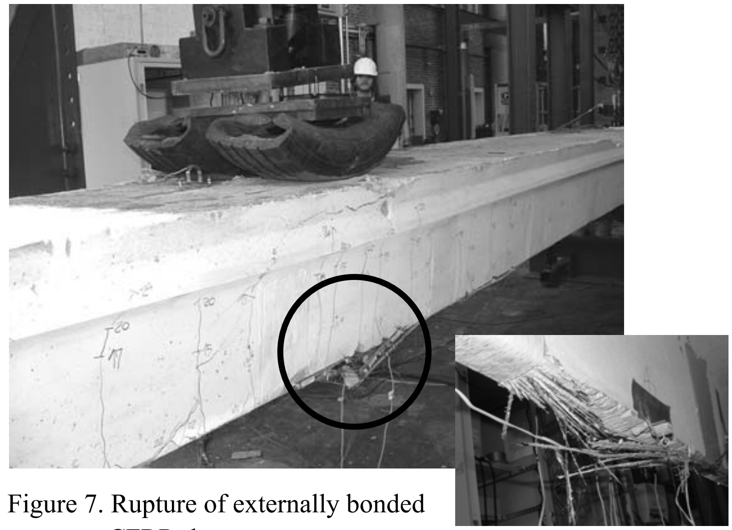

Figure 7. Rupture of externally bonded CFRP sheets

Figure 8. shows the applied load versus crack width relationships for the tested specimens. Comparable crack widths were observed for all the strengthened specimens. Strengthening of prestressed concrete members using FRP systems decreased the crack width at ultimate by 20-40 percent in comparison to the control specimen.

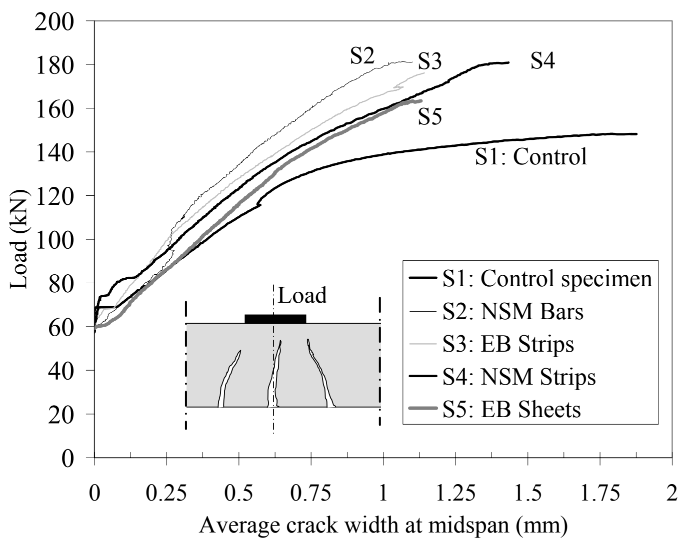

Figure 8. Average crack width for the prestressed concrete girders

3 ANALYTICAL MODELING

3.1 *Non-linear finite element model*

The control specimen as well as the specimen strengthened with NSM CFRP bars (S1 and S2) were analyzed using non-linear finite element program. The finite element modeling described in this paper was conducted using the ANACAP program (Version 2.1). ANACAP software employs the classical incremental theory of plasticity that relates the increment of plastic strain to the state of stresses and stress increment (James, 1997). The concrete material is modeled by the smeared cracking methodology in which progressive cracking is assumed to be distributed over an entire element (Gerstle, 1981). The reinforcement is assumed to be distributed throughout the concrete element. The analysis is conducted using an incremental-iterative solution procedure, in which the load is incrementally increased. Within each increment equilibrium is iteratively achieved. At the end of each step, the ANACAP program adjusts the stiffness matrix to reflect the nonlinear changes in the stiffness. Verification of the ANACAP program using independent experimental results can be found elsewhere (Hassan et al., 2000).

3.2 *Modeling of the C-Channels*

Figure 9 shows the mesh dimensions used in the finite element model. Due to symmetry, one quarter of the girder was modeled as shown in Figure 9. The concrete was modeled using 20-node isoparametric brick elements. Each node has three translational degrees of freedom. The compressive strength of the concrete as well as the effective prestressing in the strands were set identical to the measured values, given in Table 2. The wheel load was applied as uniform pressure acting on the top of the girder. The load was applied gradually using step-by-step analysis up to failure.

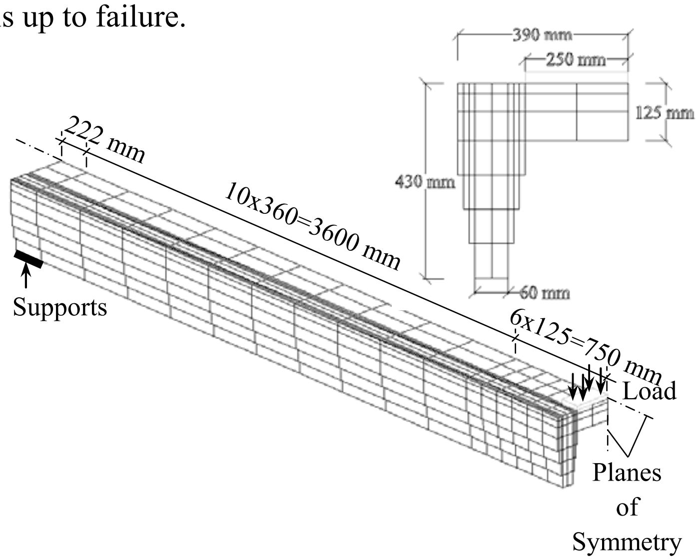

Figure 9. Mesh dimensions used in the finite element model

The predicted load-deflection behavior for specimens S1 and S2 compared to the experimental results is shown in Figure 10. The predicted values matched the experimental results with a sufficient accuracy. Failure occurred due to crushing of the concrete at the mid-span section. The predicted failure loads were within one percent of the measured values for both specimens. The tensile strain in NSM CFRP bars at a distance of 600 mm from the mid-span section was predicted using non-linear finite element analysis. The results were compared to the measured values as shown in Figure 11.

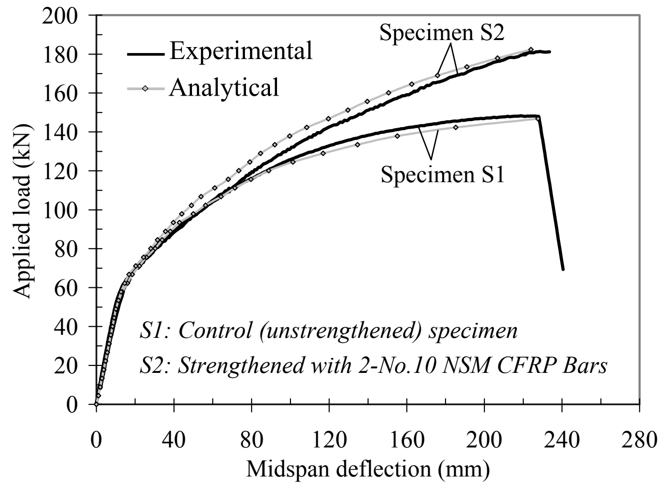

Figure 10. Predicted and measured load-deflection behavior of the C-channels

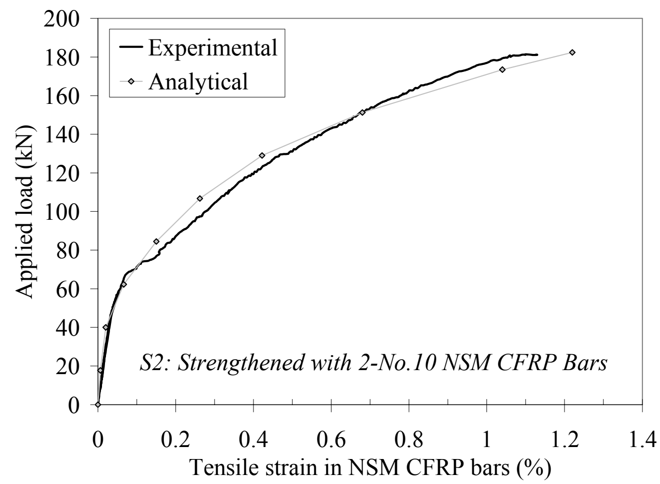

Figure 11. Predicted and measured load-tensile strain behavior of NSM CFRP bars

The predicted values compared well with the experimental results up to a load level of 150 kN, beyond which the experimental results were slightly less than the predicted values. This could be attributed to possible slippage of the NSM CFRP bars from the surrounding adhesive. Such a phenomenon was not considered in the analysis as a perfect bond was always assumed between the concrete and the reinforcement.

4 COST-EFFECTIVENESS ANALYSIS

The benefits of NSM CFRP reinforcement for strengthening were clearly highlighted in the previous sections. The advantage of using this system in comparison to the EB system is obvious. Nevertheless, it may not be the most cost-effective solution due to the time consumed in cutting of the grooves and other installation requirements.

To closely resemble field conditions, the strengthening was conducted while the girders were placed side by side as they would be on a bridge, supported by a steel substructure provided by the

NCDOT. The strengthening started in February when nighttime temperatures were below those recommended for curing of adhesive by its manufacturer. Therefore a plastic enclosure was provided as well as propane heaters. This cost was assumed to be similar for all types of bridges repaired under these conditions and was not included in the analysis.

To determine the cost-effectiveness of each strengthening technique the following items were considered: (1) labor cost of the professional FRP applicators, (2) time taken to complete all tasks, (3) material costs and (4) equipment used for strengthening. The material costs include all primers, adhesives and CFRP that may be required in a field application. Equipment items included in Table 4 are the rental of the sandblasting pot, compressor and the purchase of two 180mm diamond saw blades used to cut the grooves. All other equipment (such as grinders, mixers, safety equipment, etc) is either assumed to be provided by the contractor or used equally in each of the strengthening systems. These values in Tables 3 & 4 should be used for comparison purposes only.

Table 3. Strengthening Cost - Labor

Task	NSM Bars	NSM Strips	EB Strips	EB Sheets
	hrs	hrs	hrs	hrs
Groove Cutting	11	11	-	-
Surface Preparation	1.25	1.25	3.88	3.88
Lay-up	5.63	6.13	10	9.75
Total / Beam	17.9	18.4	13.9	13.6
Total / meter*	2.17	2.23	1.69	1.66
$ / meter**	97.65	100.35	76.05	74.70

* Based on a strengthened length of 8.23m
** Based on an assumed labor cost of $45 / hour

Table 4. Strengthening Cost – Materials / Equipment / Summary

Task	NSM Bars	NSM Strips	EB Strips	EB Sheets
	$ / m	$ / m	$ / m	$ / m
Adhesive, primer, etc	21.44	21.44	16.48	8.54
CFRP	24.4	18.55	198.72	19.53
Equipment*	5.47	5.47	0.00	0.00
Sandblaster Rental	2.40	2.40	7.44	7.44
Total / meter (mat&equip)	53.72	47.87	222.65	35.51
Total cost / meter*	151.37	148.22	298.70	110.21
Cost Effectiveness**	14.5	15.5	6.4	9

* Including labor costs above
** Based on (% increase in ultimate strength) / (Cost per meter) x100

The cost analysis indicated that the most cost-effective systems (when comparing the variables described above and the percent increase in ultimate strength of the specimen) were the NSM systems. Although being more labor-intensive to install, the CFRP and adhesive are cheaper per meter than the EB systems and the percent increase in ultimate strength is greater. Of the EB systems, the CFRP sheets showed the least increase in ultimate capacity. However, the inexpensive material costs made it more cost-effective compared to the externally bonded CFRP strips.

5 CONCLUSIONS

Five 40 year old 9.14m long prestressed girders have been tested under static loading: one control and four strengthened with different CFRP systems. Based on the results, the following conclusions can be drawn:

1 The ultimate strength of prestressed concrete members can be substantially increased using FRP strengthening systems. The ultimate load carrying capacity of aged prestressed girders tested in this research program increased by as much as 23 percent in comparison to the control specimen according to the design value.
2 Serviceability could not be used as a criterion to compare the efficiency of various FRP strengthening techniques for prestressed concrete members, since negligible differences were observed among the various techniques at the service load level.
3 The selected configuration of U-wraps enhanced the behavior of the strengthened prestressed girders and delayed delamintaion of externally bonded CFRP strips and sheets.
4 Using NSM or EB FRP systems reduced the crack width at ultimate by 20-40 percent compared to the unstrengthened specimen.
5 Defining cost-effectiveness as the percent increase in ultimate capacity divided by the cost of the strengthening, the most cost-effective systems are those which utilize NSM strengthening. Externally bonded CFRP strips is the least cost-effective system compared to the other techniques.
6 The behavior of the aged unstrengthened as well as strengthened prestressed concrete girders can be well predicted using a non-linear finite element analysis.

6 ACKNOWLEDGEMENTS

The authors would like to acknowledge the support of the North Carolina Department of Transportation through Project 2004-15, National Science and Engineering Research Council of Canada and the National Council of Scientific and Technological Development, CNPq, Brazil. Several industry members made appreciated material donations: David White of the Sika Corporation and Doug Gremel of Hughes

Brothers. In addition, Structural Preservation Systems carried out the strengthening work and provided the VSL materials. The authors would also like to thank Jerry Atkinson, the technician at the Constructed Facilities Laboratory, whose help was invaluable.

7 REFERENCES

American Society for Testing and Materials, 2003. Standard Test Method for Obtaining and Testing Drilled Cores and Sawed Beams of Concrete. *ASTM C42-03*.

De Lorenzis, L.A., Nanni, A. & La Tegola, A. 2000. Flexural and Shear Strengthening of Reinforced Concrete Structures with Near Surface Mounted FRP Rods. In J. Humar and A.G. Razaqpur (eds.), *Proc., 3rd International Conference on Advanced Composite Materials in Bridges and Structures, Ottawa, Canada, 15-18 August 2000*.

De Lorenzis & Nanni, A. 2001. Characterization of FRP Rods as Near-Surface Mounted Reinforcement. *Journal of Composites for Construction* 5(2): 114-121.

Gerstle, K.H. 1981. Material modeling of Reinforced Concrete. IABSE Colloquium on Advanced Mechanics of Reinforced Concrete, Introductory Report, Delft, Netherlands, 1981.

Hassan, T., Abdelrahman, A., Tadros, G., and Rizkalla, S. 2000. FRP Reinforcing Bars For Bridge Decks, Canadian Journal for Civil Engineering 27(5): 839-849.

Hassan, Tarek & Rizkalla, Sami, 2003. Investigation of Bond in Concrete Structures Strengthened with Near Surface Mounted Carbon Fiber Reinforced Polymer Strips. Journal of Composites for Construction 7(3): 248-257.

Hassan, Tarek & Rizkalla, Sami, 2002. Flexural Strengthening of Prestressed Bridge Slabs with FRP Systems. PCI Journal, Jan 2003: 76-93.

James, R. G. 1997. ANACAP Concrete Analysis Program Theory Manual Version 2.1. Anatech Corp., San Diego, CA, 1997.

Malek, A.M., Saadatmanesh, H., & Ehsani, M.R. 1998. Prediction of Failure Load of RC Beams Strengthened with FRP Plate Due to Stress Concentration a the Plate End. ACI Structural Journal. 95(1): 142-152.

Smith, S.T. & Teng J.G. 2002. FRP Strengthened RC Beam I – Review of Debonding Strength Models. *Engineering Structures* 24(4): 385-395.

Smith, S.T. & Teng J.G. 2002. FRP Strengthened RC Beam II – Assessment of Debonding Strength Models. *Engineering Structures* 24(4): 397-417.

Takács, P. F. & Kanstad T. 2000. Strengthening prestressed concrete beams with Carbon Fiber Reinforced Polymer plates, *NTNU Report R-9-00*, Trondheim, Norway, 2000

Wu, Zhishen & Niu, Hedong 2000. Study on Debonding Failure Load of RC Beams Strengthened with FRP Sheets. *Journal of Structural Engineering*. 46(3).

Zia, P. & Kowalsky M.J. 2002. Fatigue Performance of Large-Sized Long-Span Prestressed Concrete Girders Impaired by Transverse Cracks. *Federal Highway Administration Report,* FHWA/NC/2002-024.